Optical transitions of Er^{3+} ions in $RbMgF_3$ and $RbMgF_3$:Mn

M. D. Shinn, J. C. Windscheif,* D. K. Sardar, and W. A. Sibley
Physics Department, Oklahoma State University, Stillwater, Oklahoma 74078
(Received 2 February 1982; revised manuscript received 4 June 1982)

Optical absorption, emission, and excitation spectra, as well as lifetime values, are presented for Er^{3+} ions in $RbMgF_3$. Previous workers have demonstrated that Er^{3+} ions can reside in a number of different site symmetries in crystalline hosts such as CaF_2 and CdF_2. The numerous sites in this type lattice are most likely due to compensating fluorine interstitials which are necessarily present for charge compensation. In a unit cell of $RbMgF_3$ there are two nonequivalent Mg^{2+} sites with C_{3v} symmetry. Evidence is presented in this paper that Er^{3+} ions in $RbMgF_3$ substitute for Mg^{2+} ions in both types of sites. The charge compensation is not local, which leaves the symmetry of the Er^{3+} sites unchanged. Absorption data for Er^{3+}-ion transitions in both sites are shown. Emission from Er^{3+} ions is observed from one type of site in $RbMgF_3$ and from both types of sites in $RbMgF_3$:Mn. Lifetime values for the $^4S_{3/2}$ and $^4F_{9/2}$ transitions are shorter than those normally measured in fluoride host lattices, and the emissions are quenched above 200 K. Energy migration among Er^{3+} ions and subsequent energy transfer to Mn^{2+}-ion impurities are responsible for the steady-state and transient-emission behavior.

I. INTRODUCTION

The spectra of rare-earth ions in insulators have been studied in detail over the last two decades.[1–5] In particular, the optical properties of Er^{3+} have received special attention and numerous excellent investigations have been made.[6–18] Basically, it is found that energy levels for this ion, when embedded in various crystal host lattices, are essentially the same as those for the free ion regardless of the site symmetry or the composition of the host lattice.[1] Nonetheless, there are small energy shifts and the investigations of Wright[13] and Moore and Wright[14] on CaF_2 and Ensign and Byer[18] on CdF_2 have shown numerous site symmetries for Er^{3+} in these hosts. The number of observed sites and the fact that the oscillator strengths of the transitions can vary by an order of magnitude suggest that charge-compensating fluorine interstitials play a major role in determining the observed optical properties in fluoride crystals.

In the past several years we have investigated the radiation damage properties in fluorides such as $KMgF_3$, $LiYF_4$, and $RbMgF_3$. Studies on $RbMgF_3$ doped with Mn^{2+} have shown that after irradiation and thermal annealing, F-center$-Mn^{2+}$ pairs are formed and the oscillator strengths of the Mn^{2+} transitions are enhanced by factors of about 10^5.[19,20] Erbium exhibits a weak oscillator strength. If F-center$-Er^{3+}$ pairs could be formed the oscillator strengths of the erbium transitions might be enhanced, which would increase its usefulness in laser or up-conversion devices. This paper deals with the optical properties of Er^{3+} ions in unirradiated $RbMgF_3$ and $RbMgF_3$:Mn. In a following paper,[20] the optical properties of Er^{3+} ions in electron irradiated $RbMgF_3$ will be reported.

Crystals of $RbMgF_3$ have six Mg^{2+} ions per unit cell. All Mg^{2+} sites have C_{3v} symmetry, but two of the sites have equidistantly placed F^- ions making the local symmetry closer to O_h, while four of the Mg^{2+} ions are in constricted sites with F^- ions at nonequidistant points. The necessary charge compensation for Er^{3+} ions could be by fluorine interstitials as in CaF_2, by Rb^+ vacancies, or by alkali ions in Mg^{2+} sites.[21] Since the samples were not intentionally doped with alkali ions, this last possibility seems remote. One purpose of this paper is to discover if Er^{3+} populates both types of Mg^{2+} sites in $RbMgF_3$ and to determine the energy levels of the ions in these sites. A second purpose is the detailed evaluation of the $^4S_{3/2}\rightarrow{}^4I_{15/2}$ and $^4S_{3/2}\rightarrow{}^4I_{13/2}$ emission.

Flaherty and DiBartolo,[6,7] Wilson *et al.*,[9] and Iverson and Sibley[22] have all reported that the luminescence transitions associated with the $^4S_{3/2}$ level are quenched in MnF_2 and $RbMnF_3$ crystals. The energy-gap$-$dependence analysis for rare-earth ions developed by Weber[3,5] and an evaluation using the theory of Struck and Fonger[23,24] predict a non-

radiative multiphonon emission rate of about 300 s^{-1} at 10–15 K for this transition. If the radiative lifetime is less than 3 ms, emission should be observable; otherwise the transition will be quenched by multiphonon emission. Weber[3] found the lifetime of the $^4S_{3/2}$ transition to be 1 ms in LaF_3 at 77 K. Renfro *et al.*[15] reported a lifetime of 650 μs for this transition in $LiYF_4$. If the observed lifetime of this transition in $RbMgF_3$ is similar to those in LaF_3 and $LiYF_4$ (much faster than the predicted 3 ms nonradiative rate) then it would be reasonable to infer, assuming Er^{3+} has similar properties in $RbMgF_3$ and $RbMnF_3$, that rapid energy transfer from the Er^{3+} $^4S_{3/2}$ level to the Mn^{2+} $^4T_{1g}$ level is responsible for the lack of $^4S_{3/2}$ emission in MnF_2 and $RbMnF_3$. This would verify the mechanism postulated by Flaherty and DiBartolo,[6,7] Wilson *et al.*,[9] and Iverson and Sibley.[22]

II. EXPERIMENTAL METHODS

The crystals used in this study were grown by Martin of the Oklahoma State University Crystal Growth Facility. The crystals were grown in an inert atmosphere using the Bridgeman technique. A small amount of NH_4HF_2 was added to the starting material as an oxygen getter. Several types of crystals were prepared. One crystal was grown with 1 wt.% Er^{3+} added. One crystal with 1 at.% Er^{3+} and another crystal with 0.5 at.% Er^{3+} were grown as well as one crystal with 1 at.% Mn^{2+} and 1 at.% Er^{3+}. The concentration of Er^{3+} in the resulting crystals was not uniform. The concentration of Er^{3+} in the 1 wt.% doped crystal varied from 9000 to 400 ppm. Nonetheless it is important to note that experimental evidence[20] suggests that there is a random distribution of the Er^{3+} ions in the samples. In addition to the above crystals, several specimens of a $KMgF_3$ crystal which was grown with 0.1 at.% Er^{3+} in the melt at the same facility were obtained for comparison with the $RbMgF_3$:Er samples.

For low-temperature measurements, a Sulfrian helium cryostat, or a CTI Cryodyne Cryocooler with a resistance heater which allowed temperature control within ± 1 K over the range 13–300 K were utilized. Optical absorption measurements were made using a Cary 14 spectrophotometer with either 0–0.1 or 0–1.0 OD (optical density) slidewires. Emission from Er^{3+} occurs over a wide spectral range. Therefore, several different detectors were employed; cooled EMI 9556 or RCA C31034 photomultiplier tubes (PMT's) for the visible, a RCA 7102 PMT at dry-ice temperature for the near infrared, and a cooled Optoelectronics OTC-22-53 PbS cell for the infrared. Emission and excitation spectra measurements were made by exciting the samples with light from a 75-W xenon-arc lamp which had been passed through a 0.22-m Spex monochromator. The fluorescence was focused into a 0.8-m Spex monochromator and mirrors were used to route the light emerging from the exit slit to the appropriate detector. The signal from the detector was preamplified and passed to a lock-in amplifier that was synchronized with a variable-speed light chopper in the excitation beam. The output of the lock-in amplifier may be displayed on an *X-Y* recorder or stored in a Nicholet Model 1070 signal averager. Lifetime measurements were made by storing the preamplified signal in the Nicholet signal averager. For fast lifetimes the preamplified signal was sent to a Biomation 610 B transient recorder and stored in the Nicholet signal averager. This system allowed lifetimes as short as 10 μs to be measured.

III. EXPERIMENTAL RESULTS

A figure showing the hexagonal structure of $RbMgF_3$, and giving the unit cell dimensions, is depicted elsewhere.[19] The Mg^{2+} sites, where it is ex-

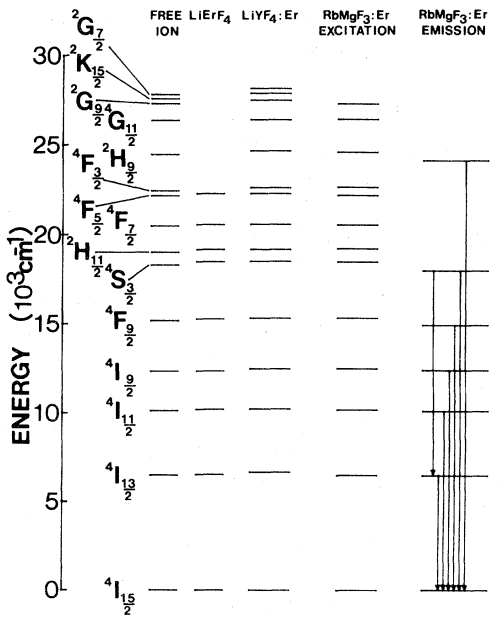

FIG. 1. Energy-level diagram of Er^{3+} as a free ion (Ref. 1), in $LiErF_4$ (Ref. 12), in $LiYF_4$ (Ref. 15), and for the present work.

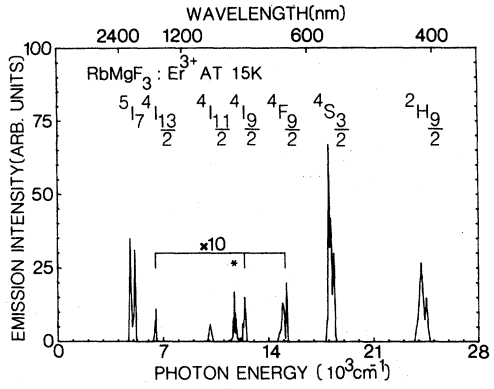

FIG. 2. Emission spectrum of $RbMgF_3$:Er. The band marked * corresponds to the $^4S_{3/2} \rightarrow {}^4I_{13/2}$ transition. The intensities of the bands marked $\times 10$ were increased by this amount.

pected the Er^{3+} ions will substitute, have similar surroundings to those in $KMgF_3$ or $RbMnF_3$, i.e., there are six fluorine neighbors. However, the Mg^{2+} ions are in two nonequivalent C_{3v} sites. In $RbMnF_3$ the Mn^{2+} ions are all in O_h symmetry sites. As mentioned earlier, charge compensation for the Er^{3+} ion could be achieved by a Rb^+ vacancy, or an interstitial fluorine ion. In any case the $4f$ electrons of Er^{3+} are shielded by the outer $5s$ and $5p$ electrons and are not easily perturbed by the ligands. Evidence that this is the case is shown in Fig. 1. This figure indicates that the energy levels for Er^{3+} are essentially those of the free ion, regardless of whether charge compensation is or is not needed. The energy levels for $RbMgF_3$:Er shown in Fig. 1 were determined from the low-temperature emission and excitation data shown in Figs. 2 and 3. In Fig. 2 the emission peak marked with a star is the transition $^4S_{3/2} \rightarrow {}^4I_{13/2}$ and the double-peaked emission near 5000 cm^{-1} is due to

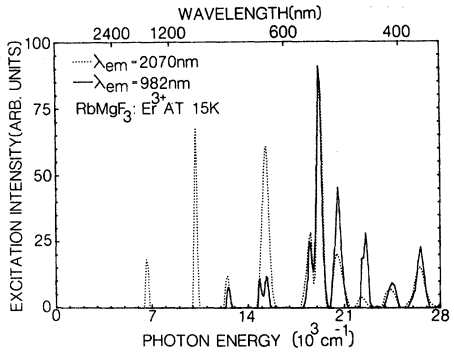

FIG. 3. Excitation spectrum of $RbMgF_3$:Er. Transitions monitored were the Er^{3+} $^4I_{11/2} \rightarrow {}^4I_{15/2}$ (982 nm) and the Ho^{3+} $^5I_7 \rightarrow {}^5I_8$ (2070 nm).

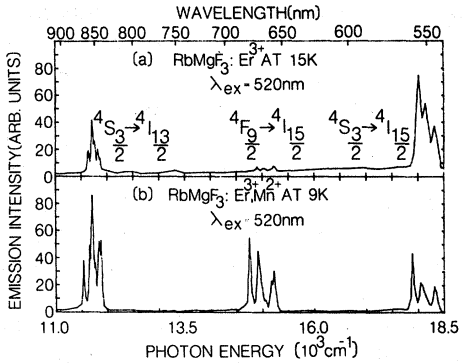

FIG. 4. Emission of Er^{3+} in (a) $RbMgF_3$ and (b) $RbMgF_3$:Mn in the visible and near-infrared region of the spectrum. Resolution in both cases is 2 nm.

Ho^{3+} present as an impurity in the 1-wt.% Er^{3+}-doped sample. The excitation spectrum shown in Fig. 3 was taken using the Er^{3+} $^4I_{11/2} \rightarrow {}^4I_{15/2}$ and the Ho^{3+} $^5I_7 \rightarrow {}^5I_8$ emissions. The excitation spectrum for the Ho^{3+} emission contained many bands due to Er^{3+} and allowed the accurate determination of the position of the $^4I_{13/2}$ level. In the low-resolution case, the excitation spectra showed no difference between the $RbMgF_3$:Er and the $RbMgF_3$:Er,Mn samples. However, when the $^2H_{11/2}$ absorption band is excited the emission from a sample of $RbMgF_3$:Er differs from the emission of a sample of $RbMgF_3$:Er,Mn as shown in Figs. 4(a) and 4(b), respectively. Note that the

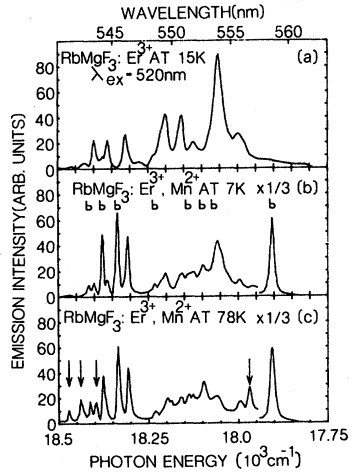

FIG. 5. $^4S_{3/2} \rightarrow {}^4I_{15/2}$ emission of Er^{3+} in (a) $RbMgF_3$ and (b), (c) $RbMgF_3$:Mn. The letters and arrows above the bands are explained in the text. In all cases the $^2H_{11/2}$ level (520 nm) was excited. Resolution: (a) 2.5 Å, (b) 1.8 Å, (c) 1.0 Å. The intensities of the bands marked $\times \frac{1}{3}$ were reduced by this amount.

$^4F_{9/2} \rightarrow {}^4I_{15/2}$ emission is larger in proportion to the $^4S_{3/2} \rightarrow {}^4I_{15/2}$ emission in the $RbMgF_3$:Er,Mn samples. Also the $^4S_{3/2} \rightarrow {}^4I_{15/2}$ emission intensities are different for the two types of samples.

In order to determine the crystal-field splitting of the $^4I_{15/2}$ ground state of Er^{3+} in $RbMgF_3$, low-temperature high-resolution emission spectra were obtained for the $^4S_{3/2} \rightarrow {}^4I_{15/2}$ and $^4F_{9/2} \rightarrow {}^4I_{15/2}$ transitions in both Er- and Er,Mn-doped samples. For a site of C_{3v} symmetry the $^4I_{15/2}$ multiplet is split into eight levels by the noncubic crystal field. This splitting should be evident in the emission spectra. Figure 5(a) is the emission spectrum for the $^4S_{3/2} \rightarrow {}^4I_{15/2}$ transition in $RbMgF_3$:Er. Figures 5(b) and 5(c) show the emission spectra for the same transition in $RbMgF_3$:Er,Mn at 7 K and 78 K, respectively. Comparison of Fig. 5(a) with Fig. 5(b) immediately shows that a second series of lines denoted "*b*" appears in the $^4S_{3/2} \rightarrow {}^4I_{15/2}$ emission in $RbMgF_3$:Er,Mn that is not in the emission from $RbMgF_3$:Er. The arrows in Fig. 5(c) indicate a set of emissions which appear as the sample is warmed. This set of emissions is separated from the *b* series of emissions by 62 cm^{-1}. Figure 6(a) is the emission spectrum for the $^4F_{9/2} \rightarrow {}^4I_{15/2}$ transition in $RbMgF_3$:Er. Figure 6(b) is the emission spectra for the same transition in $RbMgF_3$:Er,Mn.

The intense transition from the $^4S_{3/2}$ level to the $^4I_{13/2}$ level in the low-temperature emission spectrum was measured for both types of samples to evaluate the crystal-field splitting. The $^4I_{13/2}$ multiplet is split into seven levels in a noncubic crystal-

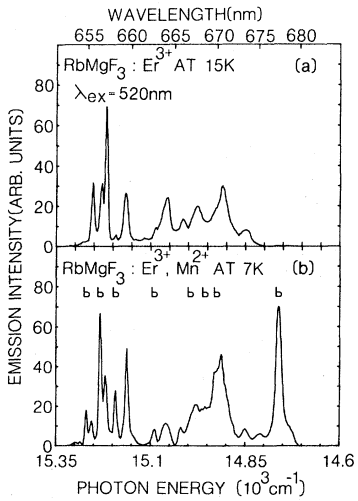

FIG. 6. $^4F_{9/2} \rightarrow {}^4I_{15/2}$ emission of Er^{3+} in (a) $RbMgF_3$ and (b) $RbMgF_3$:Mn. The letters above the bands are explained in the text. In both cases the $^2H_{11/2}$ level (520 nm) was excited. Resolution: (a) 3.0 Å, (b) 1.3 Å.

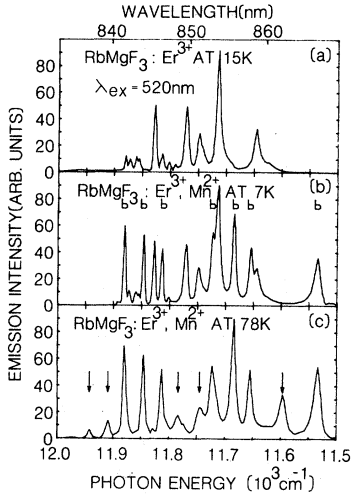

FIG. 7. $^4S_{3/2} \rightarrow {}^4I_{13/2}$ emission of Er^{3+} in (a) $RbMgF_3$ and (b), (c) $RbMgF_3$. The letters and arrows above the bands are explained in the text. In all cases the $^2H_{11/2}$ level (520 nm) was excited. Resolution: (a) 4.0 Å, (b) and (c) 3.5 Å.

line field. The spectra obtained are shown in Figs. 7(a)–7(c). Figure 7(c) shows that as the temperature increases once again a set of emissions, marked by arrows, appears 62 cm^{-1} to higher energy from the lowest-temperature *b* emissions in Fig. 7(b).

In principle the low-temperature absorption spectra of Er^{3+} can be used to determine how many types of sites are occupied by the Er^{3+} ion. This assumes the absorption bands do not greatly overlap, and the Er^{3+} concentration for each of the site symmetries is sufficient for detection. The $^4S_{3/2}$ multiplet is the simplest excited state of Er^{3+}, since it is split into only two levels in a noncubic crystalline field. The absorption spectrum of the $^4I_{15/2} \rightarrow {}^4S_{3/2}$ transition in $RbMgF_3$:Er,Mn at three

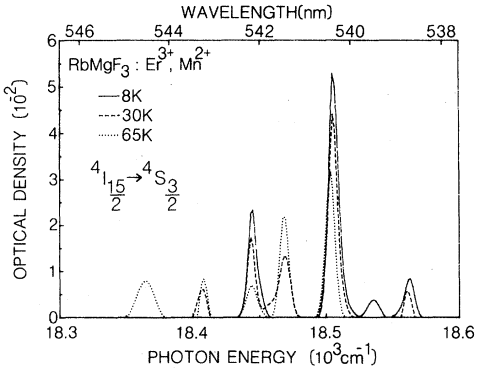

FIG. 8. Absorption spectra of the $^4S_{3/2}$ level in $RbMgF_3$:Er,Mn at 8 K (solid line), 30 K (dashed line), and 65 K (dotted line). The sample thickness was approximately 2 mm.

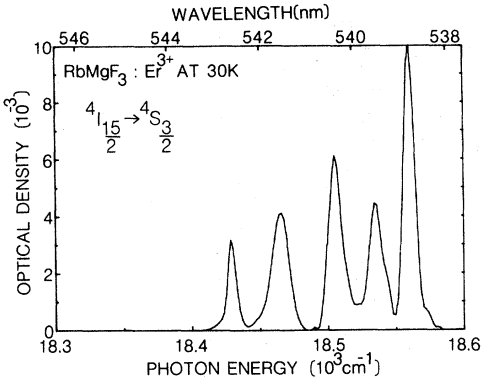

FIG. 9. Absorption spectrum of the $^4S_{3/2}$ level in $RbMgF_3$:Er at 30 K. The sample thickness was 7 mm.

different temperatures is shown in Fig. 8. At 8 K the absorption spectrum (solid line) consists of four bands. At this temperature only the lowest level of the $^4I_{15/2}$ multiplet is populated, so only two absorption bands for the $^4I_{15/2} \rightarrow {}^4S_{3/2}$ transition are possible for each Er^{3+} site. Since two sets of two lines are found, it appears Er^{3+} in $RbMgF_3$:Mn occupies both types of Mg^{2+} sites. In order to assign the observed lines to ions in a particular site the temperature dependence of the spectrum was measured. As the temperature is raised to 30 and 65 K, new absorption bands appear at 35 and 78 cm^{-1} on the high-energy side of the absorption bands at 18 504 cm^{-1} (540.42 nm) and 18 444 cm^{-1} (542.19 nm) as portrayed in Fig. 8. These new bands are the result of the Boltzmann population of the next two highest levels in the $^4I_{15/2}$ ground-state multiplet for the Er^{3+} ions in one of the sites. The energy separation of the bands at 18 504 and 18 444 cm^{-1} is 60 cm^{-1}. This agrees, within experimental error, with the observed energy separation between the emission bands marked with arrows and the *b* bands in Figs. 5(c) and 7(c). Note that in Fig. 5(b)

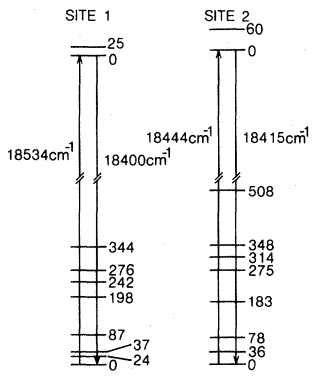

FIG. 10. Energy splittings of the $^4S_{3/2}$ and $^4I_{15/2}$ multiplets for Er^{3+} in site 1 and site 2 in $RbMgF_3$.

the difference in energy between the first three *b* bands, at 18 418, 18 382, and 18 340 cm^{-1} is 36 and 78 cm^{-1}. This matches the energy splittings of the first three levels of the $^4I_{15/2}$ multiplet, for Er^{3+} in one of the two possible sites, which were derived from the absorption data in Fig. 8. The corresponding transitions for the $^4F_{9/2} \rightarrow {}^4I_{15/2}$ emission, shown in Fig. 6(b), have splittings of 36 and 77 cm^{-1}, which are again in excellent agreement with the absorption data. From these observations it is clear that the absorption bands at 18 504 and 18 444 cm^{-1} characterize the $^4S_{3/2}$ excited state for one site, with the *b* emissions in Fig. 5(b) arising from the transitions to the ground state for Er^{3+} in that site. Similarly, the remaining absorption and emission bands, shown in Figs. 8 and 5(b), respectively, are due to Er^{3+} in the other site.

The absorption spectrum of a $RbMgF_3$:Er sample at 30 K is depicted in Fig. 9. Comparison with Fig. 8 shows that absorption occurs at the same energies, although the relative intensities of the absorption bands are different. Also, the bands at 18 407 and 18 444 cm^{-1} were unmeasurable due to the lower erbium concentration in the sample. Nevertheless, Er^{3+} clearly occupies both sites in $RbMgF_3$, although emission is from one site. For convenience, the site from which the Er^{3+}-ion luminesces in $RbMgF_3$ shall be referred to as site 1. The other Er^{3+} site shall be referred to as site 2. From these data the energy splittings of the $^4I_{15/2}$ ground state and the $^4S_{3/2}$ excited state of Er^{3+} in both sites were tabulated. This information is shown in Fig. 10.

From the data illustrated in Fig. 7 for the $^4S_{3/2} \rightarrow {}^4I_{13/2}$ emission the $^4I_{13/2}$ energy levels can be determined. The Er^{3+} ions in site 2 have levels split by 0, 34, 67, 158, 195, 225, and 346 cm^{-1}. The site-1 ion levels are more difficult to obtain but five of these are at 11 827, 11 770, 11 748, 11 713, and 11 643 cm^{-1}. The absorption and emission lines for $RbMgF_3$:Er,Mn are shown in Tables I and II, respectively.

Lifetime measurements provide useful information about an ion and its surroundings. Weber[3] showed that in LaF_3:Er^{3+} a relationship exists for the magnitude of the energy gap between adjacent levels and the lifetime. As the energy gap decreases, so does the lifetime. For energy gaps greater than or approximately equal to 3000 cm^{-1} the emission is essentially totally radiative, giving temperature-independent lifetimes at low temperatures while for energy gaps less than 1600 cm^{-1} nonradiative decay is so dominant that fluorescence is quenched. For energy gaps intermediate in magnitude between

TABLE I. Absorption of Er^{3+} at 9 K in $RbMgF_3$:Mn. All transitions originate from the $^4I_{15/2}$ level. Measurements are accurate to ± 2 cm^{-1}. If known, the specific Er^{3+} site is listed.

Transition	Energy (cm^{-1})	Wavelength (nm)	Site	Transition	Energy (cm^{-1})	Wavelength (nm)	Site
$^4F_{7/2}$	20735	482.3		$^4F_{9/2}$	15534	643.8	
	20680	483.6			15469	646.5	
	20659	484.1			15406	649.1	
	20625	484.8			15343	651.8	
	20588	485.8			15296	653.8	
	20560	486.4					
	20494	487.9		$^4I_{13/2}$	6762	1478.9	
					6730	1485.9	2
$^2H_{11/2}$	19414	515.1			6695	1493.8	2
	19391	515.7			6656	1502.3	2
	19369	516.3			6623	1510.0	
	19332	517.3			6606	1513.8	
	19318	517.7			6568	1522.6	2
	19254	519.4			6535	1530.2	2
	19233	519.9			6500	1538.4	2
	19187	512.2					
	19147	522.3					
$^2S_{3/2}$	18563	538.7	1				
	18536	539.5	1				
	18505	540.4	2				
	18443	542.2	2				

these two extremes, multiphonon emission becomes more important causing the lifetime to be temperature dependent at low temperatures. A careful series of lifetime measurements were made on all the more intense emission lines from $RbMgF_3$:Er and $RbMgF_3$:Er,Mn. The lifetimes of $^4S_{3/2}\rightarrow{}^4I_{15/2}$, $^4S_{3/2}\rightarrow{}^4I_{13/2}$, and $^4F_{9/2}\rightarrow{}^4I_{15/2}$ emissions of Er^{3+} in $RbMgF_3$, where only site 1 luminesces, were measured to compare with the lifetime values obtained for that site in $RbMgF_3$:Er,Mn. The lifetimes measured at 15 K are listed in Table III. Estimated errors for single exponential lifetimes are $\sim 5\%$. For double exponential lifetimes the errors for the longer lifetimes are $\sim 5\%$ and $\sim 20\%$ for the shorter lifetimes. For all lifetime measurements the $^2H_{11/2}$ level was excited. Note that the $^4S_{3/2}$ lifetimes for site 1 in $RbMgF_3$, and the same site in $RbMgF_3$:Mn, have essentially the same single lifetime, while these lifetimes in site 2 in $RbMgF_3$:Mn have double lifetimes. Within experimental error, the $^4F_{9/2}$ lifetime was a single exponential, and had the same value for both sites. However, the initial

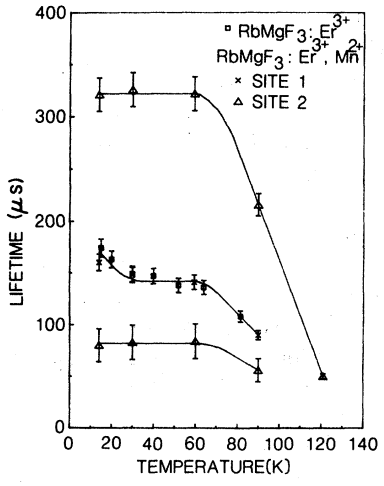

FIG. 11. Temperature dependence of the Er^{3+} $^4S_{3/2}$ lifetime in $RbMgF_3$ and $RbMgF_3$:Mn.

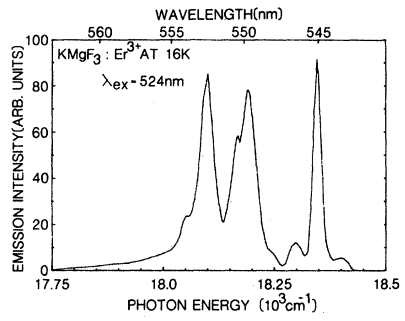

FIG. 12. $^4S_{3/2}\rightarrow{}^4I_{15/2}$ emission of Er^{3+} in $KMgF_3$. Resolution: 5 Å.

TABLE II. Emission of Er^{3+} in $RbMgF_3$:Mn at 9 K. Measurements are accurate to ± 2 cm^{-1}.

Transition	Energy (cm^{-1})	Wavelength (nm)	Site	Transition	Energy (cm^{-1})	Wavelength (nm)	Site
$^2H_{9/2}\rightarrow{}^4I_{15/2}$	24 510	408		$^4I_{9/2}\rightarrow{}^4I_{15/2}$	12 407	806	
	24 155	414					
				$^4S_{3/2}\rightarrow{}^4I_{13/2}$	11 882	841.6	2
$^4S_{3/2}\rightarrow{}^4I_{15/2}$	18 415	543.0	2		11 874	842.2	
	18 400	543.5	1		11 862	843.0	
	18 379	544.1	2		11 856	843.5	
	18 376	544.2	1		11 847	844.1	2
	18 363	544.6	1		11 829	845.4	1
	18 337	545.4	2		11 812	846.6	2
	18 313	546.1	1		11 802	847.3	
	18 232	548.5	2		11 772	849.5	1
	18 202	549.4	1		11 750	851.1	1
	18 158	550.7	1		11 724	853.0	2
	18 140	551.3	2		11 714	853.6	1
	18 124	551.8	1		11 683	855.9	2
	18 101	552.5	2		11 656	857.9	2
	18 067	553.5	2		11 645	858.7	1
	18 056	553.8	1		11 536	866.9	2
	17 995	555.7					
	17 907	558.4	2	$^4I_{11/2}\rightarrow{}^4I_{15/2}$	10 101	990	
$^4F_{9/2}\rightarrow{}^4I_{15/2}$	15 270	654.9	2	$^4I_{13/2}\rightarrow{}^4I_{15/2}$	6494	1540	
	15 256	655.5	1				
	15 233	656.5	2				
	15 231	656.5	1				
	15 220	657.1	1				
	15 193	658.2	2				
	15.163	659.5	1				
	15 090	662.7	2				
	15 060	664.0	1				
	15 020	665.8	1				
	14 995	666.9	2				
	14 980	667.6	1				
	14 957	668.6	2				
	14 926	670.0	2				
	14 913	670.6	1				
	14 848	673.5					
	14 762	677.4	2				

decay of the site-1 luminescence deviated from a simple single exponential behavior. No such behavior was observed for the site-2 luminescence decay. In addition to these measurements the lifetime of the $^4I_{13/2}$ transition in $RbMgF_3$ was measured and found to be 13 ms.

The temperature dependence of the $^4S_{3/2}$ lifetime is displayed in Fig. 11. Note that the site-1 lifetimes in $RbMgF_3$ and $RbMgF_3$:Mn have the same temperature dependence. The lifetimes decrease above 60 K. The integrated intensities of the emission bands for both sites show similar behavior. At room temperature, luminescence is not observed from either site 1 or site 2, whereas in LaF_3, $LiYF_4$, CaF_2, or CdF_2, $^4S_{3/2}$ luminescence is observed above room temperature.[3,14,15,18] The $^4I_{13/2}$ luminescence is temperature independent from 15 to 300 K. This observation is consistent with the earlier studies.[3,15,22]

Preliminary studies were made on a sample of $KMgF_3$ grown with 0.1 at.% Er^{3+} added to the melt. This crystal also contained 10–50 ppm of inadvertently added Mn^{2+}. If Er^{3+} substitutes for Mg^{2+}, charge compensation is required. If the charge compensation is not local the Er^{3+} ion will be in a site of O_h symmetry. For Er^{3+} in a site of

TABLE III. Lifetimes of Er^{3+} in $RbMgF_3$ and other fluoride crystals.

Material	$^4S_{3/2}$	$^4F_{9/2}$	$^4I_{11/2}$	$^4I_{13/2}$
LaF_3 (Ref. 3) $T=77$ K	1 ms	750 μs	11 ms	13 ms
$LiYF_4$ (Ref. 15) $T=4.2$ K	650 μs	650 μs	7 ms	14.6 ms
MnF_2 (Ref. 7) $T=4.2$ K		270 μs	10 ms	22 ms
$RbMnF_3$ (Ref. 22) $T=4.2$ K		42 μs	9 ms	28 ms
$RbMgF_3$ $T=15$ K	174 μs	340 μs		13 ms
$RbMgF_3$:Mn $T=15$ K Site 1	160 μs	340 μs		
Site 2	80 μs, 320 μs	340 μs		

cubic symmetry, the crystal field splits both the $^4I_{15/2}$ and $^4I_{13/2}$ multiplets into five levels. The high-resolution emission spectra of the $^4S_{3/2}\rightarrow{}^4I_{15/2}$ and $^4S_{3/2}\rightarrow{}^4I_{13/2}$ transitions of Er^{3+} in $KMgF_3$ are shown in Figs. 12 and 13, respectively. Both spectra have no more than five bands, indicating that the Er^{3+} ion is in a cubic site symmetry. The $^4F_{9/2}\rightarrow{}^4I_{15/2}$ transition was measured and found to exhibit five bands. This suggests the charge compensation is predominantly nonlocal. This conclusion is supported by the investigations of Abraham *et al.*[25] on the electron paramagnetic resonance of Er^{3+} in $KMgF_3$.

Several other measurements on $KMgF_3$:Er were also made. When the $^2H_{11/2}$ level was excited, the emission spectrum in the visible region looked much like that shown in Fig. 4(b), with the $^4F_{9/2}\rightarrow{}^4I_{15/2}$ emission easily detected. When the $^2H_{11/2}$ level was excited, the lifetime of the $^4S_{3/2}$ emission was 71 μs, and the lifetime of the $^4F_{9/2}$ emission was 161 μs. No lifetime-temperature-dependence measurements were made; however, it should be noted that luminescence from either the $^4S_{3/2}$ or $^4F_{9/2}$ level was not detected at room temperature.

IV. DISCUSSION

The experiments on the emission of Er^{3+} in $KMgF_3$ show that Er^{3+} is in a site of O_h symmetry.

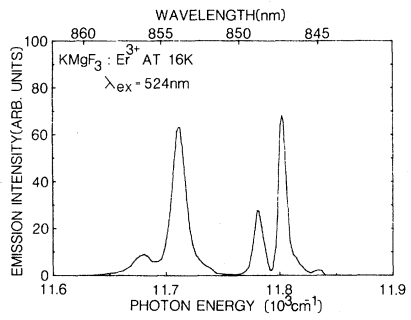

FIG. 13. $^4S_{3/2}\rightarrow{}^4I_{13/2}$ emission of Er^{3+} in $KMgF_3$. Resolution: 4 Å.

This is achieved only if the Er^{3+} ion substitutes for the Mg^{2+} ion, and the required charge compensation is nonlocal. Abraham *et al.*[25] found that in $KMgF_3$ the majority of Er^{3+} ions were in cubic sites with nonlocal charge compensation. However, a small concentration of Er^{3+} ions in noncubic sites was observed. Their interpretation was that the charge compensation was local and provided by K^+ and Mg^{2+} vacancies.

The data for $KMgF_3$ imply that the compensation for Er^{3+} ions in $RbMgF_3$ would be nonlocal, leaving the site symmetries of the Mg^{2+} ions for which they substitute unchanged. Thus the optical properties of Er^{3+} in the two nonequivalent C_{3v} sites and their interactions are characterizable. Studies on optical properties of Er^{3+} in other fluoride lattices such as CaF_2 are complicated by the different types of compensation and the large number of site symmetries which exist. The $RbMgF_3$ lattice is ideal for studying the optical properties of Er^{3+} since only two sites exist and the charge-compensating defects are not next neighbors.

The $^4S_{3/2}$ lifetime for $RbMgF_3$:Er is not characteristic of the radiative rate observed in other fluoride crystals. The magnitude of the lifetime is much shorter. This is illustrated in Table III, where the $^4S_{3/2}$ lifetime and other lifetimes of interest for $RbMgF_3$:Er and $RbMgF_3$:Er,Mn are compared with lifetimes of Er^{3+} in other fluoride crystals. Also, in $RbMgF_3$ and $KMgF_3$ the $^4S_{3/2}$ lifetime decreases with a corresponding quenching of the luminescence intensity above 60 K. In many other crystals this emission is easily observed at room temperature. We propose that this behavior is due to energy migration among Er^{3+} ions to impurity ions which act as quenching centers. We found that all of our $RbMgF_3$:Er and $KMgF_3$:Er crystals contained about (10–50)-ppm Mn^{2+}. Owing to the large overlap of the $^4T_{1g}$ level of Mn^{2+} with the $^4S_{3/2}$ level of Er^{3+}, resonant-energy transfer is probable. This overlap is believed responsible for the quenching of the $^4S_{3/2}$ emission in MnF_2:Er and $RbMnF_3$:Er.[6,7,22,9] This previous research found

that the Er^{3+} excitation spectrum contained Mn^{2+} bands, showing that Er^{3+}-Mn^{2+} energy transfer occurs. Figures 4(a) and 4(b) show that as the Mn^{2+} concentration is increased from 50 to greater than or about 1000 ppm the $^4F_{9/2}$ intensity also increases, giving direct evidence that the energy-transfer process,

$$^4S_{3/2}\ (Er^{3+}) \rightarrow {}^4T_{1g}\ (Mn^{2+}) \rightarrow {}^4F_{9/2}\ (Er^{3+}) ,$$

occurs at low Er^{3+} and Mn^{2+} concentrations.

Additional evidence that energy migration occurs among Er^{3+} ions at low concentrations was provided by experiments performed on the 1-wt. % Er^{3+}-doped $RbMgF_3$ sample. The emission spectrum from this crystal showed an intense double-peaked band at 5115 cm^{-1} (1955 nm) and 4831 cm^{-1} (2070 nm). This emission is almost exactly the same as that reported by Johnson *et al.*[26] for $CaMO_4$:0.75 at. % Er^{3+}, 0.5 at. % Ho^{3+} and by Karpick and DiBartolo[27] for Y_3Al_2 $(Al0_4)_3$:2.0 at. % Er^{3+}, 0.2 % Ho^{3+}. We conclude that this emission is due to energy transfer from the $^4I_{13/2}$ level of Er^{3+} to the $^5I_7$ level of Ho^{3+}. A careful search failed to detect absorption bands due to Ho^{3+} in this sample. Assuming an oscillator strength of 10^{-6} (Ref. 28) the estimated Ho^{3+} concentration can therefore be no more than 100 ppm. An energy-transfer process similar to that proposed by Dexter and Schulman[29] must occur. The excited Er^{3+} ions transfer their energy to unexcited Er^{3+} ions until an Er^{3+} ion near a Ho^{3+} ion transfers its energy to the Ho^{3+} ion. This allows a large number of Er^{3+} ions to contribute to the Ho^{3+} luminescence and results in intense Ho^{3+} emission.

When the Er^{3+} energy levels have no overlap with the Mn^{2+} energy levels and the difference between energy levels cannot be compensated by the emission of several phonons, which occurs when Er^{3+} transfers to Ho^{3+}, then the relaxation process for Er^{3+} in $RbMgF_3$ should be the same as in other fluoride crystals. The validity of this statement can be checked by comparing the value of the $^4I_{13/2}$ lifetime for the various crystals listed in Table III. The 12000 cm^{-1} energy gap between the $^4T_{1g}$ Mn^{2+} level and the $^4I_{13/2}$ Er^{3+} level makes energy transfer directly between the two levels highly improbable. The values in Table III indicate that the $^4I_{13/2}$ lifetime is relatively unchanged in most of the cases shown.

Having established that in these crystals the Er^{3+} ions transfer energy among themselves and eventually to Mn^{2+} and Ho^{3+} ions as well, it is possible to explain the observed luminescence spectra and to make a tentative assignment of the source ions to the site-1 and site-2 specific lattice sites. It was shown earlier that, although Er^{3+} occupies both possible Mg^{2+} sites in $RbMgF_3$ only the Er^{3+} in site 1 luminesces when the $^2H_{11/2}$ level is excited. The excitation source excites Er^{3+} ions in both sites 1 and 2 to the $^2H_{11/2}$ level where, due to the small gap between the $^2H_{11/2}$ and $^4S_{3/2}$ levels, nonradiative decay to the $^4S_{3/2}$ level occurs. Figure 10 shows that the relaxed excited state for the $^4S_{3/2}$ Er^{3+} level in site 1 is lower by 15 cm^{-1} than for Er^{3+} in site 2. The site-2 Er^{3+} ions thus transfer their excitation to other Er^{3+} ions until the excitation reaches an Er^{3+} ion in site 1. This Er^{3+} ion can relax either radiatively or nonradiatively, or transfer the excitation to another site-1 Er^{3+} ion but it is not likely to transfer the excitation back to a site-2 ion. Hence, luminescence from the $^4S_{3/2}$ level in $RbMgF_3$:Er occurs only from site 1. Moreover, nonradiative transitions to lower levels involve only Er^{3+} ions in site 1.

This explanation must be reconciled with the emission data for $RbMgF_3$:Er,Mn, where excitation to the $^2H_{11/2}$ level causes $^4S_{3/2}$-level luminescence from both sites. The only difference between the two types of samples is the increased Mn^{2+} concentration, thus the appearance of site-2 Er^{3+} luminescence must correlate with the Mn^{2+} concentration. This behavior may be explained once again in terms of energy migration among Er^{3+} ions and energy transfer to Mn^{2+} ions. Consider the final step in the energy-transfer process, in which an Er^{3+} ion transfers energy to a Mn^{2+} ion. If the energy transfer occurs via an electric dipole-dipole interaction the energy-transfer rate is given by[30]

$$\omega_{sa}^{DD} = (\tau_s^0)^{-1}(R_0/R)^6 ,$$

where τ_s^0 is the intrinsic lifetime of the sensitizers (Er^{3+}) and where R_0 is the critical interaction distance between the sensitizer and the activator (Mn^{2+}), beyond which no transfer occurs. The assumption that the interaction is electric dipole-dipole is made on the basis that higher-order multipole processes would be ineffective due to the long distance between Er^{3+} and Mn^{2+} ions, and by the conclusion of Parke and Cole[31] that the interaction between Mn^{2+} and Er^{3+} ions in glass is electric dipole-dipole.

In the case of Er^{3+} in $RbMgF_3$:Mn it appears that R_0 is different for Er^{3+} in the two sites, with R_0 for Er^{3+} in site 1 being greater than R_0 for Er^{3+} in site 2. For low Mn^{2+} concentrations the average distance between Er^{3+} in site 2 and Mn^{2+} ions is too great for energy transfer to occur and it is more likely to follow the migration process to

Er^{3+} ions in site 1 proposed earlier. As the Mn^{2+} concentration increases the average Mn^{2+}-Er^{3+} separation decreases, until energy transfer may occur directly from Er^{3+} ions in site 2 to Mn^{2+} ions. The lifetime data for the $^4S_{3/2}$ emission in $RbMgF_3$:Er,Mn supports this explanation. As stated earlier, the site-1 Er^{3+} ions decay exponentially with a lifetime which is shorter than normally seen. This is the fast diffusion-relaxation case Weber has described.[32] In $RbMgF_3$:Er,Mn, energy migration is rapid among site-1 Er^{3+} ions due to their small separation, compared to the critical-transfer distance R_0, so that variations in transfer rates for different Er^{3+}-Mn^{2+} pairs are averaged and the site-1 Er^{3+} system exhibits simple exponential decay. The $^4S_{3/2}$ emission from site-2 Er^{3+} ions exhibits a more complicated luminescence decay. In this case we have attempted to fit the entire decay curve to two exponentials. As stated earlier, the shorter-lifetime exponential, which describes the initial decay fits the data more poorly, with higher error as a consequence. A comparison of our data with that given by Weber for the diffusion-limited relaxation case indicates that the same type of process is occurring. Again, this is consistent with our explanation. As the site-2 Er^{3+} to Mn^{2+} distance decreases with higher Mn^{2+} concentration eventually it will reach the point where it is more likely to transfer energy directly to a Mn^{2+} ion. Owing to the smaller value of R_0 for site-2 Er^{3+} ions not all the site-2 Er^{3+} ions are within range for direct transfer, those close enough do transfer while those Er^{3+} ions further away must first transfer their energy to other Er^{3+} ions until transfer to a Mn^{2+} ion results. Thus the excitation energy may be thought of as diffusing from these more distantly placed sensitizer ions until it is in the vicinity of an acceptor ion. There are several theories which attempt to explain the result of this type of relaxation on the luminescence decay. All of them predict a decay more complicated than simple exponential.[32–34] No attempt to fit the data to one of these theories was made.

Having proposed mechanisms for the observed steady-state and transient luminescence only the assignment of the two sites to specific lattice configurations remains. Our assignment is based on Fig. 10, which shows that the $^4S_{3/2}$ and $^4I_{15/2}$ J manifolds have smaller Stark splittings for site 1 than for site 2. It is reasonable to assume that the less constricted environment of the Mg^{2+} site with the equidistantly spaced F^- ions will result in a smaller crystalline Stark field than the more constricted environment of the other site. This is consistent with the splitting observed in $KMgF_3$:Er, which has the same Mg-F ligand distance (2.81 Å) as the less constricted site. On this basis, we assign the site-1 emission and absorption to Er^{3+} ions in the less constricted Mg^{2+} sites, and the site-2 emission and absorption to Er^{3+} ions in the more constricted Mg^{2+} sites.

V. SUMMARY

The optical absorption, emission, and excitation spectra and the temperature dependence of the luminescence lifetimes have been measured for Er^{3+}-doped $RbMgF_3$ and $RbMgF_3$:Mn. A preliminary study of $KMgF_3$:Er was also made. The data indicate that Er^{3+} substitutes for Mg^{2+} in these crystals and the necessary charge compensation is nonlocal, leaving the site symmetry unchanged. In $RbMgF_3$ there are two nonequivalent sites, both with C_{3v} symmetry, and Er^{3+} resides in both sites.

Our investigations show that energy migration occurs among Er^{3+} ions at the relatively low concentrations (<1 at. %) present in the crystals. It was also found that the presence of Mn^{2+}, even at concentrations as low as 10—50 ppm, resulted in efficient resonant-energy transfer from the Er^{3+} $^4S_{3/2}$ level to the Mn^{2+} $^4T_{1g}$ level. This energy transfer causes the luminescence decay to be rapid and results in luminescence intensity and decay quenching above 60 K. The energy-transfer characteristics are different for Er^{3+} in each site. If the Mn^{2+} concentration is very low (~ 50 ppm) only Er^{3+} in one site luminesces, while in samples containing 1000 ppm or more of Mn^{2+}, both Er^{3+} sites luminesce. A similar energy-transfer process occurs when trace amounts of Ho^{3+} are present.

ACKNOWLEDGMENTS

The authors would like to thank R. C. Powell, J. J. Martin, and R. Orbach for many helpful discussions. G. S. Dixon provided the $KMgF_3$:Er samples. We would also like to thank J. C. Chandler of the Computing and Information Systems department at Oklahoma State University for his nonlinear least-squares computer program. This work was supported by NSF Grant No. DMR 81-05017.

*Present address: Fraunhofer-Institut für Angewandte Festkörperphysik, Eckerstrasse 4, D-7800 Freiburg, I. Br. West Germany.

[1]G. H. Dieke, *Spectra and Energy Levels of Rare-Earth Ions in Crystals* (Interscience, New York, 1968).

[2]S. Hufner, *Optical Spectra of Transparent Rare Earth Compounds* (Academic, New York, 1978).

[3]M. J. Weber, Phys. Rev. 157, 262 (1967).

[4]M. J. Weber, in *Physics of Quantum Electronics,* edited by P. L. Kelley, B. Lax, and P. E. Tannewald (McGraw-Hill, New York, 1966), pp. 350–360.

[5]L. A. Riseberg and M. J. Weber, in *Progress in Optics,* edited by E. Wolf (Elsevier, New York, 1976), Vol. 14, p. 89.

[6]J. M. Flaherty and B. DiBartolo, Phys. Rev. B 8, 5232 (1973).

[7]J. M. Flaherty and B. DiBartolo, J. Lumin. 8, 51 (1973).

[8]J. M. Flaherty and B. DiBartolo, *Colloques Internationaux C.N.R.S.* (Centre National de la Recherche Scientifique, Paris, 1977), Vol. 255, p. 191.

[9]B. A. Wilson, W. M. Yen, J. Hagerty, and G. F. Imbush, Phys. Rev. B 19, 4238 (1979).

[10]M. R. Brown, K. G. Roots, and W. A. Shand, J. Phys. C 2, 593 (1969).

[11]M. V. Petrov and A. M. Tkachuk, Opt. Spektrosk. 45, 147 (1978).

[12]H. P. Christensen, Phys. Rev. B 19, 6564 (1979).

[13]J. C. Wright, in *Radiationless Processes in Molecules and Condensed Phases,* Vol. 15 of *Topics in Applied Physics,* edited by F. K. Kong (Springer, Berlin, 1976), p. 239.

[14]D. S. Moore and J. C. Wright, J. Chem. Phys. 74, 1626 (1981).

[15]G. M. Renfro, J. C. Windscheif, W. A. Sibley, and R. F. Belt, J. Lumin. 22, 51 (1980).

[16]I. V. Mochalov, Phys. Status Solidi A 55, 79 (1979).

[17]A. A. Kaminskii, in *Proceedings of the International Conference on Lasers, 1980,* edited by C. B. Collins (STS Press, McLean, Virginia, 1981), p. 382.

[18]J. C. Ensign and N. E. Byer, Phys. Rev. B 6, 3227 (1972).

[19]N. Koumvakalis and W. A. Sibley, Phys. Rev. B 13, 4509 (1976).

[20]D. K. Sardar, M. D. Shinn, and W. A. Sibley, following paper, Phys. Rev. B 26, xxxx (1982).

[21]M. Hirano and S. Shionoya, J. Phys. Soc. Jpn. 28, 926 (1970).

[22]M. V. Iverson and W. A. Sibley, Phys. Rev. B 21, 2522 (1980).

[23]C. W. Struck and W. H. Fonger, J. Lumin. 10, 1 (1975).

[24]C. W. Struck and W. H. Fonger, J. Lumin. 14, 253 (1976).

[25]M. M. Abraham, C. B. Finch, J. L. Kolopus, and J. T. Lewis, Phys. Rev. B 3, 2855 (1971).

[26]L. F. Johnson, L. G. Van Uitert, J. J. Rubin, and R. A. Thomas, Phys. Rev. 133, A494 (1964).

[27]J. T. Karpick and B. DiBartolo, J. Lumin. 4, 309 (1971).

[28]M. J. Weber, T. E. Varitimos, V. L. Donlan, and G. T. Surratt, J. Chem. Phys. 57, 562 (1972).

[29]D. L. Dexter and J. H. Schulman, J. Chem. Phys. 22, 1063 (1954).

[30]R. C. Powell and G. Blasse, in *Structure and Bonding,* edited by J. D. Dunitz, J. B. Goodenough, P. Hemmerich, J. A. Ibers, C. K. Jorgensen, J. B. Neilands, D. Reinen, and R. J. P. Williams (Springer, Berlin, 1980), Vol. 42, p. 49.

[31]S. Parke and E. Cole, Phys. Chem. Glasses 12, 125 (1971).

[32]M. J. Weber, Phys. Rev. B 4, 2932 (1971).

[33]Z. G. Soos and R. C. Powell, Phys. Rev. B 6, 4032 (1972).

[34]H. C. Chow and R. C. Powell, Phys. Rev. B 21, 3785 (1980).